

Experimental report

08/07/2016

Proposal: 5-24-553

Council: 10/2014

Title: High temperature in situ NPD study of crystal structure and phase stability of high TE performance phases: $\text{Cu}_{12-x}\text{Ni}_x\text{Sb}_4\text{S}_{13}$ and $\text{Cu}_4\text{Sn}_7\text{S}_{16}$

Research area: Materials

This proposal is a new proposal

Main proposer: Pierric LEMOINE

Experimental team: Cedric BOURGES
Emmanuel GUILMEAU
Pierric LEMOINE

Local contacts: Vivian NASSIF

Samples: $\text{Cu}_{12}\text{Sb}_4\text{S}_{13}$
 $\text{Cu}_{10.4}\text{Ni}_{1.6}\text{Sb}_4\text{S}_{13}$
 $\text{Cu}_4\text{Sn}_7\text{S}_{16}$
 $\text{Cs}_2\text{Mo}_6(\text{Cl},\text{Br})_{14}$
 $\text{Ti}_{1-x}\text{Cr}_x\text{S}_2$
 $\text{Cu}_{26-x}\text{Zn}_x\text{V}_2\text{Sn}_6\text{S}_{32}$

Instrument	Requested days	Allocated days	From	To
D1B	4	4	02/08/2015	06/08/2015

Abstract:

A recent study has revealed the beneficial role of Ni on thermoelectric (TE) properties, purity and stability of the $\text{Cu}_{12-x}\text{Ni}_x\text{Sb}_4\text{S}_{13}$ tetrahedrites. The results have also shown the existence of an important kinetic effect on the phase stability at high temperature. Unfortunately, the similar atomic numbers of Cu and Ni atoms do not allow to determine accurately the crystal structure from Rietveld refinement of the XRD patterns, and the characterization of the associated kinetic effect is limited by the flux of the laboratory X-Ray tube. In parallel, we have also shown that the $\text{Cu}_4\text{Sn}_7\text{S}_{16}$ compound exhibits very low intrinsic thermal conductivity related to its complex crystal structure, and, depending of the synthesis method, evidences either a semiconducting or a metallic behavior, suggesting modification of element stoichiometry and sites occupancy, which are not detected by both powder XRD and EDX analyses. In order to determine more precisely the thermal evolution of both crystal structure and chemical composition of these very interesting TE materials and to better understand the associated electric properties, we need high temperature in situ neutron powder diffraction data.

Experimental report on the proposal 5-24-553: *High temperature in situ neutron powder diffraction study of crystal structure and phase stability of high thermoelectric performance phases: $\text{Cu}_{12-x}\text{Ni}_x\text{Sb}_4\text{S}_{13}$ and $\text{Cu}_4\text{Sn}_7\text{S}_{16}$.*

P. Lemoine^[1], C. Bourgès^[2], E. Guilmeau^[2], V. Nassif^[3]

^[1] Institut des Sciences Chimiques de Rennes, UMR-CNRS 6226, 263 av du général Leclerc, CS 74205, 35042 Rennes Cedex, France

^[2] Laboratoire CRISMAT, UMR-CNRS 6508, ENSICAEN, 6 bd du maréchal Juin, 14050 Caen Cedex 4, France

^[3] Institut Néel, UPR-CNRS/UGA 2940, 25 rue des Martyrs, BP 166, 38042 Grenoble Cedex 9, France

1. Introduction

Recently, copper-containing ternary sulphides have been attracting much attention for thermoelectric applications because most of the main components comply the actual requirements of low cost, earth abundant, and less toxicity. A non-exhaustive list includes *p*-type tetrahedrite $\text{Cu}_{12-x}\text{Tr}_x\text{Sb}_4\text{S}_{13}$ ($ZT \sim 0.8$ @ 700K) with $\text{Tr} = \text{Mn, Fe, Co, Ni, Zn}$ ($x \leq 2$) [1-8], colusite $\text{Cu}_{26}\text{V}_2\text{Sn}_6\text{S}_{32}$ ($ZT \sim 0.56$ @ 663K) [9-11], bornite Cu_5FeS_4 ($ZT \sim 0.55$ @ 550K) [12,13], Cu_2SnS_3 ($ZT \sim 0.56$ @ 750K) [14], $\text{Cu}_2\text{ZnSnS}_4$ ($ZT \sim 0.35$ @ 700K) [15,16], or *n*-type $\text{Cu}_4\text{Sn}_7\text{S}_{16}$ ($ZT \sim 0.21$ @ 700K) [17]. A common feature of tetrahedrite, colusite, bornite and $\text{Cu}_4\text{Sn}_7\text{S}_{16}$ phases is their intrinsically low thermal conductivities κ originating from high structural complexities (Fig. 1), *i.e.* large number of atoms per unit cell [18] and large Grüneisen parameter. [3] In addition, low-energy vibration mode of Cu atom out of the $[\text{CuS}_3]$ triangular planar unit in tetrahedrites explains its ultra-low thermal conductivity [2,4,11]. Same phenomena was supposed in $\text{Cu}_4\text{Sn}_7\text{S}_{16}$ [17]. In the case of the *p*-type $\text{Cu}_{26}\text{V}_2\text{Sn}_6\text{S}_{32}$ colusite, the low lattice thermal conductivity value of 0.4 W/m K at 300K was attributed to the structural complexity and mass difference between Cu, V and Sn atoms [9].

In order to explain the high thermoelectric properties of these materials, a perfect knowledge of the crystal structure is necessary. In complement to X-rays diffraction and transmission electron microscopy, neutron powder diffraction is used to determine accurately (i) the crystal structure and (ii) the phase stability at high temperature of these TE materials. Finally, neutron powder diffraction have been carried out at low temperature on $\text{Cu}_{12}\text{Sb}_4\text{S}_{13}$ in order to explain the metal-semiconductor transition observed at $T_t = 85$ K [19].

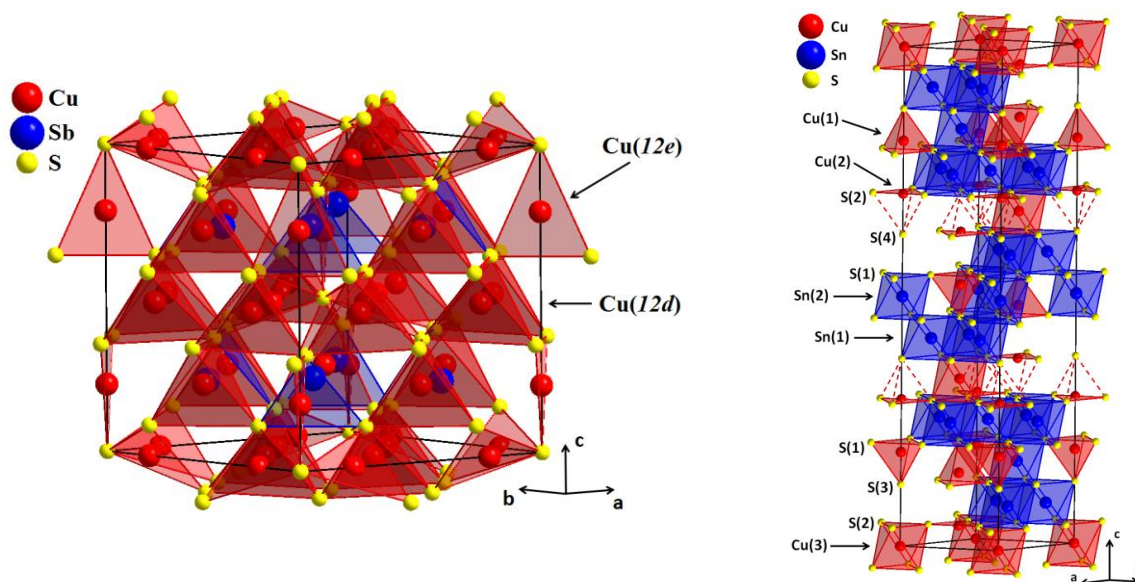


Fig. 1: Crystal structure representations of $\text{Cu}_{12}\text{Sb}_4\text{S}_{13}$ (left) and $\text{Cu}_4\text{Sn}_7\text{S}_{16}$ (right).

2. Neutron diffraction results

2.1. Tetrahedrites

Neutron diffraction patterns of $\text{Cu}_{12}\text{Sb}_4\text{S}_{13}$ have been recorded at 150 K, 50 K, and 1.4 K in order to explain the metal-semiconductor transition observed at $T_t = 85$ K [19]. The neutron pattern recorded at 150 K evidences an exsolution of the $\text{Cu}_{12}\text{Sb}_4\text{S}_{13}$ tetrahedrite phase and the presence of famatinite Cu_3SbS_4 phase (space group $I-42m$) as impurity (Fig. 2). Exsolution on synthetic un-substituted tetrahedrite leading to copper poor ($\text{Cu}_{\sim 12}\text{Sb}_4\text{S}_{13}$) and copper rich ($\text{Cu}_{\sim 14}\text{Sb}_4\text{S}_{13}$) phases [20] on one hand, and difficulty to prepare single-phase synthetic $\text{Cu}_{12}\text{Sb}_4\text{S}_{13}$ tetrahedrite [8]

on the other hand were already reported. The cubic structure (space group $I-43m$) and the cell parameters range for copper poor ($a_1 = 10.289(1) \text{ \AA}$) and copper rich ($a_2 = 10.391(1) \text{ \AA}$) tetrahedrites are confirmed at 150 K.

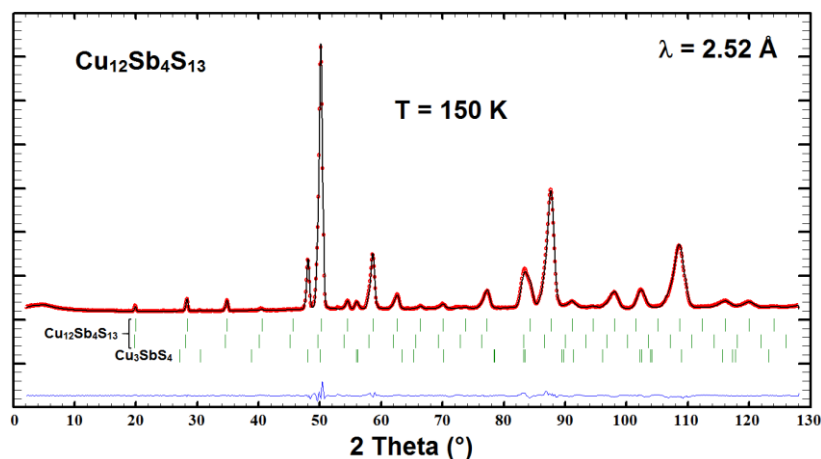


Fig. 2: Refinement of the neutron powder diffraction pattern of $\text{Cu}_{12}\text{Sb}_4\text{S}_{13}$ at 150 K with $\lambda = 2.52 \text{ \AA}$.

The neutron pattern recorded at 50 K (*i.e.* below T_1) is slightly different to that recorded at 150 K (*i.e.* above T_1), confirming the very recently reported structural phase transition of $\text{Cu}_{12}\text{Sb}_4\text{S}_{13}$ [23,24]. However, the structural transition leads to very weak modifications (Fig. 3), suggesting a superstructure induces by a symmetry lost from the highly symmetric cubic structure to a tetragonal or orthorhombic symmetry structure below 85 K. Without structural model for the low temperature form of $\text{Cu}_{12}\text{Sb}_4\text{S}_{13}$, the neutron pattern recorded at 50 K cannot be refined. Further investigations at low temperature are currently in progress. Finally, the absence of modification between 50 K and 1.4 K (Fig. 3) suggests no long range magnetic order down to 1.4 K in $\text{Cu}_{12}\text{Sb}_4\text{S}_{13}$.

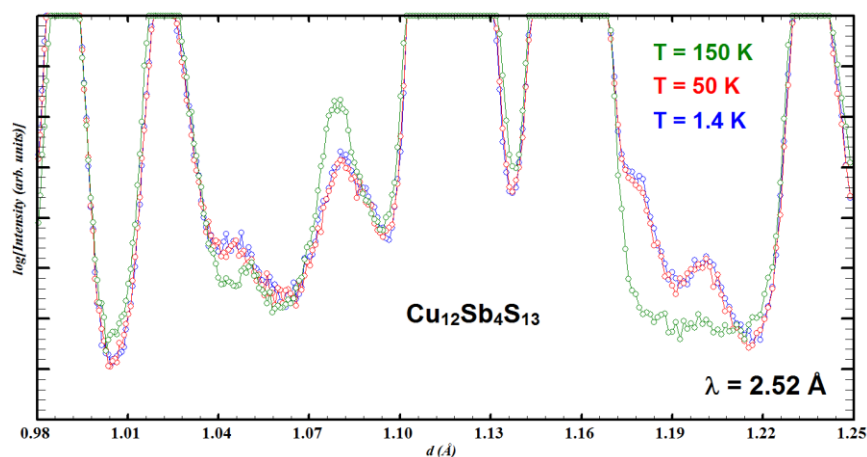


Fig. 3: Neutron diffraction patterns of $\text{Cu}_{12}\text{Sb}_4\text{S}_{13}$ recorded at 150 K (green), 50 K (red), and 1.4 K (blue).

The neutron diffraction patterns recorded at high temperature for $\text{Cu}_{12}\text{Sb}_4\text{S}_{13}$ and $\text{Cu}_{10.4}\text{Ni}_{1.6}\text{Sb}_4\text{S}_{13}$ confirm the beneficial role of nickel substituted tetrahedrite on the purity and phase stability of tetrahedrite [8]. $\text{Cu}_{12}\text{Sb}_4\text{S}_{13}$ starts to decompose through sulfur volatilization into Cu_3SbS_3 from 519°C to 548°C (Fig. 4), while $\text{Cu}_{10.4}\text{Ni}_{1.6}\text{Sb}_4\text{S}_{13}$ is stabilized up to 570°C . This study will be the subject of an upcoming publication [25].

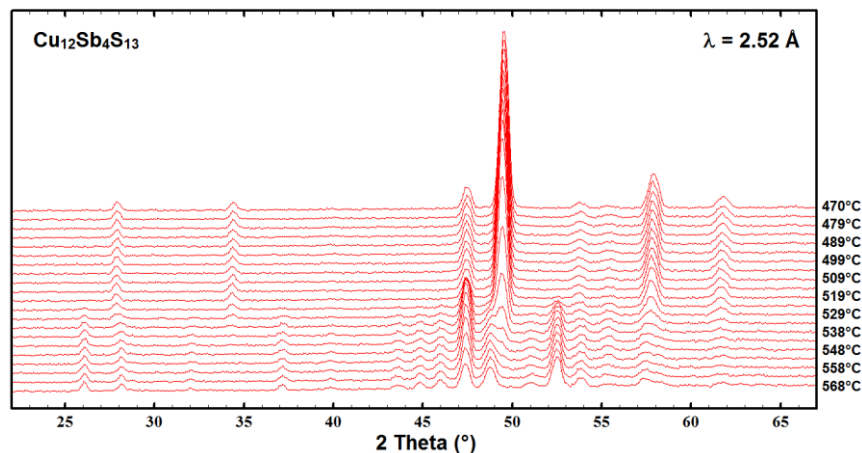


Fig. 4: Neutron thermograms of $\text{Cu}_{12}\text{Sb}_4\text{S}_{13}$.

2.2. Cu-Sn-S phases

The $\text{Cu}_4\text{Sn}_7\text{S}_{16}$ and $\text{Cu}_{26-x}\text{Zn}_x\text{V}_2\text{Sn}_6\text{S}_{32}$ ($0 \leq x \leq 2$) compounds have been characterized at 300 K in order to (i) confirm the crystal structure, (ii) determine the exact stoichiometry of the phases, and (iii) determine the preferred sites

occupation of Zn atoms. Examples of refinements are shown on Fig. 5. The interpretation of the data obtained on $\text{Cu}_4\text{Sn}_7\text{S}_{16}$ are in progress and will be the subject of an upcoming publication [26], while the results obtained on the $\text{Cu}_{26-x}\text{Zn}_x\text{V}_2\text{Sn}_6\text{S}_{32}$ ($0 \leq x \leq 2$) series will be published in Journal of Materials Chemistry C [27]. Finally, the phase stability of $\text{Cu}_4\text{Sn}_7\text{S}_{16}$ studied by *in situ* neutron powder diffraction will be also added to the publication on the phase stability of high thermoelectric performance phases [25].

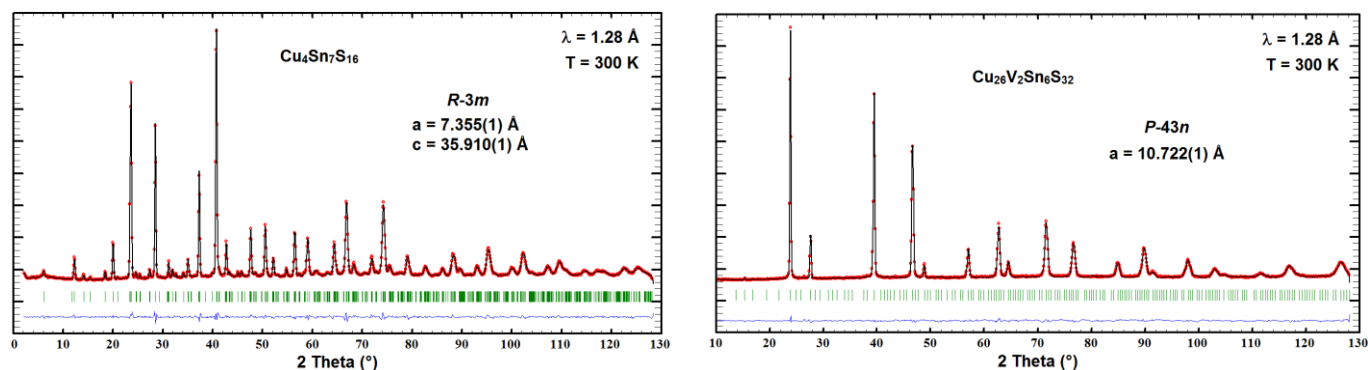


Fig. 5: Refinement of the neutron powder diffraction pattern of $\text{Cu}_4\text{Sn}_7\text{S}_{16}$ (top) and $\text{Cu}_{26}\text{V}_2\text{Sn}_6\text{S}_{32}$ (bottom) at 300 K with $\lambda = 1.28 \text{ \AA}$.

3. References

- [1] K. Suekuni, K. Tsuruta, T. Ariga, M. Koyano, *Appl. Phys. Express* 5 **2012** 4–6.
- [2] K. Suekuni, K. Tsuruta, M. Kunii, H. Nishiate, E. Nishibori, S. Maki, M. Ohta, A. Yamamoto, M. Koyano, *J. Appl. Phys.* 113 **2013** 043712.
- [3] X. Lu, D.T. Morelli, Y. Xia, F. Zhou, V. Ozolins, H. Chi, X. Zhou, C. Uher, *Adv. Energy Mater.* 3 **2013** 342–348.
- [4] E. Lara-Curzio, A.F. May, O. Delaire, M.A. McGuire, X. Lu, C.Y. Liu, E.D. Case, D.T. Morelli, *J. Appl. Phys.* 115 **2014** 193515.
- [5] R. Chetty, A. Bali, M.H. Naik, G. Rogl, P. Rogl, M. Jain, S. Suwas, R.C. Mallik, *Acta Mater.* 100 **2015** 266–274.
- [6] Y. Bouyrie, C. Candolfi, V. Ohorodniichuk, B. Malaman, A. Dauscher, J. Tobola, B. Lenoir, *J. Mater. Chem. C* 3 **2015** 10476–10487.
- [7] Y. Bouyrie, C. Candolfi, A. Dauscher, B. Malaman, B. Lenoir, *Chem. Mater.* 27 **2015** 8354–8361.
- [8] T. Barbier, P. Lemoine, S. Gascoin, O.I. Lebedev, A. Kaltzoglou, P. Vaqueiro, A.V. Powell, R.I. Smith, E. Guilmeau, *J. Alloys Compd.* 634 **2015** 253–262.
- [9] K. Suekuni, F.S. Kim, H. Nishiate, M. Ohta, H.I. Tanaka, T. Takabatake, *Appl. Phys. Lett.* 105 **2014** 132107.
- [10] K. Suekuni, F. Kim, T. Takabatake, *J. Appl. Phys.* 116 **2014** 063706.
- [11] K. Suekuni, H.I. Tanaka, F.S. Kim, K. Umeo, T. Takabatake, *J. Phys. Soc. Japan* 84 **2015** 103601.
- [12] P. Qiu, T. Zhang, Y. Qiu, X. Shi, L. Chen, *Energy Environ. Sci.* 7 **2014** 4000.
- [13] G. Guélou, A.V. Powell, P. Vaqueiro, *J. Mater. Chem. C* 3 **2015** 10624–10629.
- [14] Q. Tan, W. Sun, Z. Li, J.-F. Li, *J. Alloys Compd.* 672 **2016** 558–563.
- [15] M.L. Liu, F.Q. Huang, L.D. Chen, I.W. Chen, *Appl. Phys. Lett.* 94 **2009** 202103.
- [16] H. Yang, L.A. Jauregui, G. Zhang, Y.P. Chen, Y. Wu, *Nano Lett.* 12 **2012** 540–545.
- [17] C. Bourgès, P. Lemoine, O.I. Lebedev, R. Daou, V. Hardy, B. Malaman, E. Guilmeau, *Acta Mater.* 97 **2015** 180–190.
- [18] F.J. DiSalvo, *Science* 285 **1999** 703–706.
- [19] K. Suekuni, Y. Tomizawa, T. Ozaki, M. Koyano, *J. Appl. Phys.* 115 **2014** 143702.
- [20] E. Makovicky, B.J. Skinner, *Can. Mineral.* 16 **1978** 611–623.
- [21] J. Rodriguez-Carvajal, *Physica B* 192 **1993** 55–59.
- [22] T. Roisnel, J. Rodriguez-Carvajal, *Mater. Sci. Forum* 378–381 **2001** 118–123.
- [23] H.I. Tanaka, K. Suekuni, K. Umeo, T. Nagasaki, H. Sato, G. Kutluk, E. Nishibori, H. Kasai, T. Takabatake, *J. Phys. Soc. Jpn.* 85 **2016** 014703.
- [24] A.F. May, O. Delaire, J.L. Niedziela, E. Lara-Curzio, M.A. Susner, D.L. Abernathy, M. Kirkham, M.A. McGuire, *Phys. Rev. B* 93 **2016** 064104.
- [25] P. Lemoine *et al.*, to be published.
- [26] C. Bourgès *et al.*, to be published.
- [27] C. Bourgès, M. Gilmas, P. Lemoine, N.E. Mordvinova, O.I. Lebedev, E. Hug, V. Nassif, B. Malaman, R. Daou, E. Guilmeau, *J. Mater. Chem. C*, accepted.